23rd ABCM International Congress of Mechanical Engineering
December 6-11, 2015, Rio de Janeiro, RJ, Brazil

SUPERCRITICAL AND SUBCRITICAL BIFURCATION IN TYPICAL AEROELASTIC SECTION WITH STRUCTURAL NONLINEARITIES

D. A. Pereira
F. D. Marques
Engineering School of São Carlos – University of São Paulo
daniel.almeida.pereira@usp.br, fmarques@sc.usp.br

Abstract. *Aeroelasticity studies the mutual interaction between aerodynamic and structural dynamics loading. This physical relationship often behaves nonlinearly, causing various problems such as instabilities, limit cycle oscillations, bifurcations, and chaos that may affect aircraft operations. The objective of this work is to analyze and identify the dynamic response of a three degree of freedom airfoil section with hardening nonlinearity in the pitching stiffness and free-play nonlinearity in the control surface stiffness using the bifurcation analysis. The effect of hardening corresponds to a smooth nonlinear increasing in restoring structural loading for a given displacement. This effect is modeled here by means of the rational polynomial function while the free-play is represented by hyperbolic functions combination. Aeroelastic responses are analyzed from computational and experimental results. The numerical model is based on the classical theory for the linear unsteady aerodynamics with corrections for arbitrary motions coupled to a three degrees of freedom typical aeroelastic section. The study of the phenomena associated with the hardening, free-play, and their intensity variation effects provide ways to mitigate or circumvent any undesired responses to those behaviors. This contributes to determining safety margins for aircraft even with these nonlinearities, as fully linear systems represent major challenges to achieving, and results in very high costs.*

Keywords: *Aeroelasticity, subcritical bifurcation, supercritical bifurcation, hardening, free-play*

1. INTRODUCTION

The aeroelasticity is a multidisciplinary field of the aerospace engineering that deals with the mutual interaction between structural dynamics and non-stationary aerodynamic flow (Bisphinghoff *et al.*, 1996). Aeroelastic systems may behave nonlinearly, therefore, subject to behavior such as bifurcations, limit cycle oscillations (LCO), and chaos (Sheta *et al.*, 2002). These phenomena, whose origins are both from structural dynamics and/or from the unsteady aerodynamic loading, may be difficult to predict. The concentrated structural nonlinear effects can be incorporated into numerical models through the elastic restoring forces or moments representations. The most common types of concentrated nonlinearities representations can be given by polynomial functions, nonlinear damping effects, free-play, hysteresis, etc.

The literature is vast and many authors have been studying nonlinear aeroelastic problems in the aviation, for example, the limit cycle oscillations have caused persistent problems in many aircraft designs, such as the F-16, where Denegri and Cutchins (1997) and Chen *et al.* (1998) have observed the existence of hardening nonlinearity in wings pitching moment stiffness. O'Neil and Strganac (1998) have developed an experimental model that provides direct measurements from the typical aeroelastic section with cubic nonlinearity in the pitch and plunge motion where they examined the sensitivity of the response to system parameters. Recently, Vasconcellos *et al.* (2012, 2014) have shown that the hyperbolic tangent function combination approach for modeling discontinuous nonlinearities is appropriate for detecting different nonlinear behaviors, including the experimentally observed LCO, chaos and transitions.

It is known that the system behavior is directly related to the nonlinearities involved, for example, the system under free-play shows subcritical behavior. Figure 1 represent the classical bifurcation diagram for the supercritical and subcritical behavior where the limit cycle amplitude is plotted versus some system parameter, for example, the flight speed. In general, if the system depends on the initial condition and has different solution when the airspeed velocity is increased and decreased near the nonlinear critical velocity, the bifurcation is called subcritical, i.e. the LCOs may also exist below the flutter boundary (unstable LCO, dashed line). However, if the system are independent on the initial condition and the system stability changes only after the critical flutter velocity, the bifurcation is called supercritical and the system has only stable LCO (solid line) which sometimes is welcome because without it the LCO would instead be replaced by catastrophic flutter leading to loss of the flight vehicle (Dowell and Tang, 2002; Dowell *et al.*, 2003; Ghommem *et al.*, 2010).

Bifurcation analysis is used to indicate a quantitative and qualitative changes in the features of a system, such as the number and type of solutions, under the variation of one or more parameters on which the considered system depends on (Nayfeh and Balachandran, 1995). Abdelkefi *et al.* (2012) have analyzed changes in the system behavior of a typical

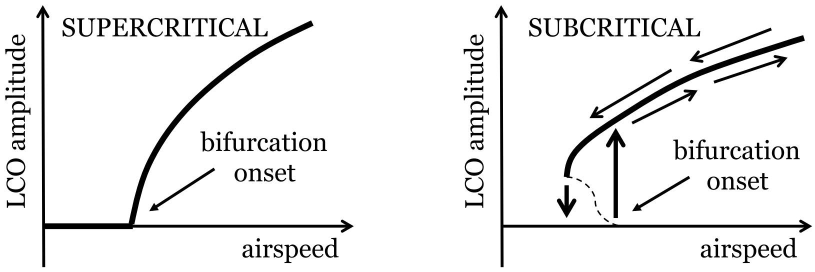

Figure 1. Supercritical bifurcation diagram leading to only stable LCO (solid line) and subcritical bifurcation diagram leading to both stable and unstable LCO (dotted line).

section presenting cubic structural nonlinearity in three degrees of freedom using bifurcation analyzes, they showed that the stability of the system are related with the influence of the different nonlinear couplings.

This work presents an investigation on the influence of the control surface free-play on the bifurcation behavior of the dynamics system when it presents a LCO induced by different hardening nonlinearity present in the pitch moment on typical aeroelastic section. The experimental and computational analyses were performed for the three degree-of-freedom airfoil and the numerical model is based on the classical theory for the unsteady aerodynamic with corrections for arbitrary motion.

2. METHODOLOGY

2.1 Mathematical Model

The mathematical model for the typical section with three degrees of freedom and semi-chord b (*cf.* Fig. 2) is derived Bisphinghoff *et al.* (1996); Theodorsen (1935), that is,

$$\begin{bmatrix} \mu_e & x_\alpha & x_\beta \\ x_\alpha & {r_\alpha}^2 & [{r_\beta}^2+(c-a)x_\beta] \\ x_\beta & [{r_\beta}^2+(c-a)x_\beta] & {r_\beta}^2 \end{bmatrix} \begin{Bmatrix} \ddot{\xi}(t) \\ \ddot{\alpha}(t) \\ \ddot{\beta}(t) \end{Bmatrix} + \begin{bmatrix} d_{1,1} & d_{1,2} & d_{1,3} \\ d_{2,1} & d_{2,2} & d_{2,3} \\ d_{3,1} & d_{3,2} & d_{3,3} \end{bmatrix} \begin{Bmatrix} \dot{\xi}(t) \\ \dot{\alpha}(t) \\ \dot{\beta}(t) \end{Bmatrix} +$$

$$\begin{bmatrix} {\omega_h}^2 & 0 & 0 \\ 0 & {r_\alpha}^2{\omega_\alpha}^2\frac{F(\alpha)}{\alpha(t)} & 0 \\ 0 & 0 & {r_\beta}^2{\omega_\beta}^2\frac{F(\beta)}{\beta(t)} \end{bmatrix} \begin{Bmatrix} \xi(t) \\ \alpha(t) \\ \beta(t) \end{Bmatrix} = \begin{Bmatrix} -L(t)/m_W b \\ M_\alpha(t)/m_W b^2 \\ M_\beta(t)/m_W b^2 \end{Bmatrix}, \quad (1)$$

where the plunge, pitch and control surface displacements are given by h, α, and β, respectively, a and c are the dimensionless distances from the elastic axis to the middle and to the surface control, U is the airspeed, x_α and x_β are the dimensionless distances from elastic axis to the center of gravity (CG) and the distance between the control surface and its CG, respectively, r_α and r_β are the dimensionless rotational inertia term about elastic axis and surface control hinge line, respectively, k_h, k_α, and k_β are the plunge, pitch and control surface stiffness, respectively, $\xi(t) = \frac{h(t)}{b}$, $\mu_e = \frac{m_T}{m_W}$, $d_{i,j}$ are the damping factors with respect to each airfoil motion and their influences (Rayleigh approach), $L(t)$ is the lift force, $M_\alpha(t)$ and $M_\beta(t)$ are the aerodynamic pitch and hinge moments, respectively, $F(\alpha)$ and $F(\beta)$ are functions related to nonlinearities applied to the stiffness.

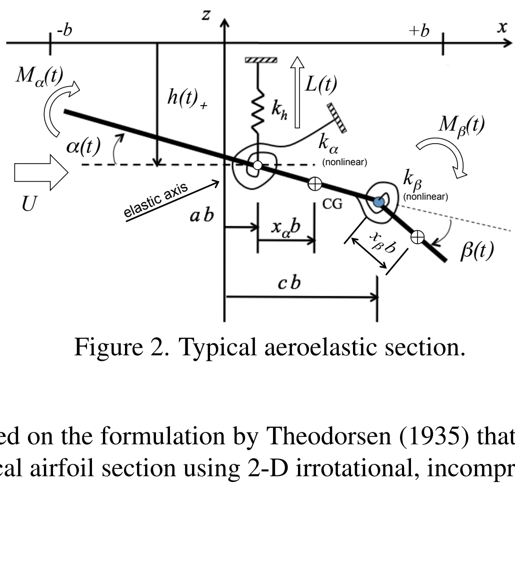

Figure 2. Typical aeroelastic section.

Aerodynamics modeling is based on the formulation by Theodorsen (1935) that presents an analytical solution to the pressure distribution around a typical airfoil section using 2-D irrotational, incompressible and potential flow and written respectively as,

$$L(t) = L^{NC} + L^{C} \ , \tag{2}$$

$$M_\alpha(t) = M_\alpha^{NC} + M_\alpha^{C} \ , \tag{3}$$

$$M_\beta(t) = M_\beta^{NC} + M_\beta^{C} \ , \tag{4}$$

where the non-circulatory terms (superscripts NC) are,

$$L^{NC} = \pi\rho b^2 \left[\ddot{h} + U\dot{\alpha} - ba\ddot{\alpha} - \frac{U}{\pi}T_4\dot{\beta} - \frac{b}{\pi}T_1\ddot{\beta}\right] \ , \tag{5}$$

$$\begin{aligned} M_\alpha^{NC} = \pi\rho b^2 \Bigg\{ & ba\ddot{h} - Ub\left(\frac{1}{2} - a\right)\dot{\alpha} - b^2\left(\frac{1}{8} + a^2\right)\ddot{\alpha} - \frac{U^2}{\pi}(T_4 + T_{10})\beta + \\ & \frac{Ub}{\pi}\left[-T_1 + T_8 + (c-a)T_4 - \frac{1}{2}T_{11}\right]\dot{\beta} + \frac{b^2}{\pi}[T_7 + (c-a)T_1]\ddot{\beta} \Bigg\} \ , \end{aligned} \tag{6}$$

$$\begin{aligned} M_\beta^{NC} = \pi\rho b^2 \Bigg\{ & \frac{b}{\pi}T_1\ddot{h} + \frac{Ub}{\pi}\left[2T_9 + T_1 - \left(a - \frac{1}{2}\right)T_4\right]\dot{\alpha} - \frac{2b^2}{\pi}T_{13}\ddot{\alpha} - \\ & \frac{U^2}{\pi^2}(T_5 - T_4T_{10})\beta + \frac{UbT_4T_{11}}{2\pi^2}\dot{\beta} + \frac{b^2T_3}{\pi^2}\ddot{\beta} \Bigg\} \ , \end{aligned} \tag{7}$$

and the circulatory terms (superscripts C) are,

$$L^{C} = 2\pi\rho UbC(k)f(t) \ , \tag{8}$$

$$M_\alpha^{C} = 2\pi\rho b^2(a + \frac{1}{2})C(k)f(t) \ , \tag{9}$$

$$M_\beta^{C} = -\rho Ub^2T_{12}C(k)f(t) \ , \tag{10}$$

where $C(k)$ is the so-called Theodorsen function and,

$$f(t) = U\alpha + \dot{h} + \dot{\alpha}b\left(\frac{1}{2} - a\right) + \frac{U}{\pi}T_{10}\beta + \frac{b}{2\pi}T_{11}\dot{\beta} \ , \tag{11}$$

is the quasi-steady term and the T-functions (T_i, for $i = 1, 2, \ldots$) are as defined in Theodorsen (1935).

The aerodynamic loading, as given from Eqs. (2) to (4), depends on the Theodorsen function $C(k)$, where $k = \frac{\omega b}{U}$ is the reduced frequency of harmonic oscillations. However, to account for arbitrary motions an alternative is to manipulate the Theodorsen function by convolution based on Duhamel formulation in the time domain (Li *et al.*, 2010). If the Wagner function is also considered, it implies that, for instance, circulatory lift term can be written as,

$$C(k)f(t) = f(0)\phi(\tau) + \int_0^\tau \frac{\partial f(\sigma)}{\partial \sigma}\phi(\tau - \sigma)d\sigma \ , \tag{12}$$

where σ is a dummy integration variable, and $\phi(\tau)$ is the Wagner function in the non-dimensional time $\tau = \frac{tu}{b}$, approximated by Sear's approach (Sears, 1940),

$$\phi(\tau) \approx c_0 - c_1e^{-c_2\tau} - c_3e^{-c_4\tau} \ , \tag{13}$$

where $c_0 = 1.0$, $c_1 = 0.165$, $c_2 = 0.0455$, $c_3 = 0.335$ and $c_4 = 0.3$.

Using integration by parts and following the state space method proposed by Lee *et al.* (1997, 2005); Li *et al.* (2010), Eq. (12) leads to a circulatory term as,

$$C(k)f(t) = (c_0 - c_1 - c_3)f(t) + c_2c_4(c_1 + c_3)\overline{x} + (c_1c_2 + c_3c_4)\dot{\overline{x}} \ , \tag{14}$$

where $\overline{x}$ and $\dot{\overline{x}}$ are augmented aerodynamic states. Substituting the Eq. (14) in Eqs. (8), (9) and (10) we obtain the circulatory aerodynamic loads for the three degrees-of-freedom.

Functions $F(\alpha)$ and $F(\beta)$ in Eq. (1) are used to feed that aeroelastic set with the respective terms to account for nonlinearities in pitch and control surface responses. Here the hardening and free-play effects are combined for that motions (*cf.* Fig. 3), being: *(i)* for pitching motion only hardening nonlinearity is considered, while, *(ii)* free-play is only affecting the control surface motion.

The hardening nonlinearity in pitching depicted in Fig. 3(a) has been obtained using the rational polynomials approximation (RP) (Li *et al.*, 2012) from the curve experimentally measured which is given by,

$$F(\alpha) = \frac{a_3\alpha^3 + a_2\alpha^2 + a_1\alpha + a_0}{b_2\alpha^2 + b_1\alpha + b_0} \quad , \tag{15}$$

where a_0 to a_3, and b_0 to b_2 are real-valued coefficients obtained numerically from measured experimental data.

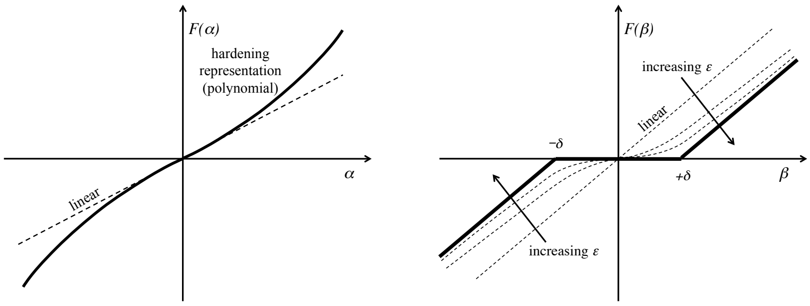

(a) Hardening representation (b) Free-play representation

Figure 3. Representations for hardening in pitching (rational polynomial approximation) and free-play in control surface deflections (hyperbolic tangent functions combination).

The free-play nonlinearity combinations of hyperbolic tangent function have been used as proposed and validated by Vasconcellos *et al.* (2014) to represent the restoring torque in the control surface. The mathematical formula for this combination is given by:

$$F(\beta) = \frac{1}{2}[1 - \tanh(\varepsilon(\beta - \beta_l))]\,(\beta - \beta_l) + \frac{1}{2}[1 - \tanh(\varepsilon(\beta - \beta_u))]\,(\beta - \beta_u)\ , \tag{16}$$

where β_l and β_u denotes the lower and the upper free-play boundary region (length of 2δ), and ε is a variable which affects the smoothness of the function, thereby determining the accuracy of the approximation (*cf.* Fig. 3(b)).

2.2 Experimental Model

The experimental apparatus comprises a rigid wing mounted along its span and it is supposed to correlate the bi-dimensional behavior of typical aeroelastic sections. The system allows three degrees of freedom (plunge, pitch, and control surface). The plunge motion is restrained by four elastic steel beams and the pitch stiffness is given by two tension springs connected by a nonlinear cam (*cf.* Fig. 5), which is responsible for the hardening nonlinearity effect. Control surface stiffness is provided by a piano wire and free-play controlled by a pair of adjustable bolts depicted in the Fig. 6. The measurements of the three degrees of freedom are done using encoders (angular and linear ones). The DSpace® system together with Simulink® are used to signals acquisition and processing. The experimental apparatus is mounted in an open-section wind tunnel ($500 \times 500 mm$) (*cf.* Fig. 4).

Figure 4. Experimental apparatus under preparation for wind tunnel tests.

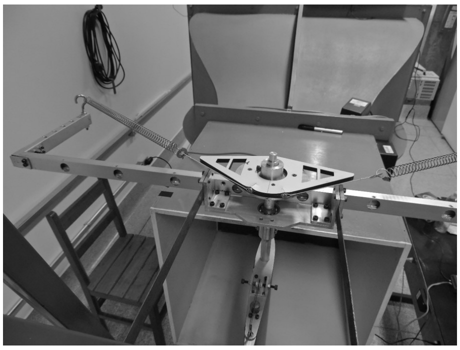
(a) Nonlinear Cam – front view

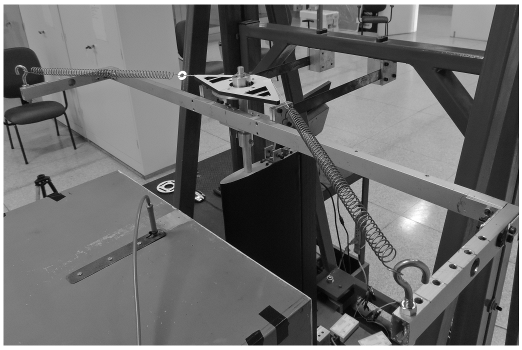
(b) Nonlinear Cam – side view

Figure 5. Details of the experimental apparatus responsible for the hardening nonlinearity.

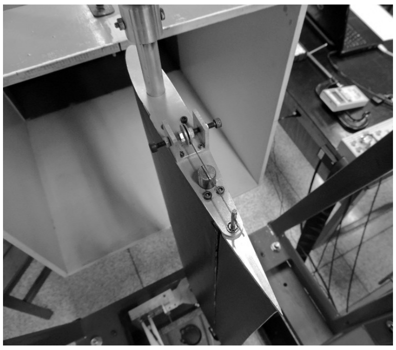
(a) Surface control set-up

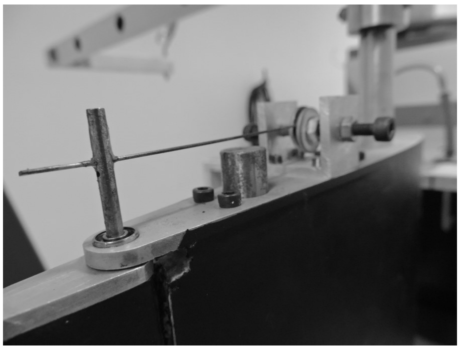
(b) Free-play adjustment device

Figure 6. Details of the experimental apparatus responsible for the free-play nonlinearity.

3. RESULTS

The aeroelastic system (*cf.* Eq. (1)) is numerically integrated using the Runge-Kutta method. The Table 1 presents the value under consideration in this work.

Table 1. Experimental values used for the numerical model.

VARIABLES	DESCRIPTION	VALUES
b	Mid-chord (m)	0.125
a	Distance from semichord to elastic axis (nondimensional)	-0.5
c	Hinge line location measured from mid-chord (nondimensional)	0.5
ρ	Air density (kg/m^3)	1.078
m_W	Wing mass (kg)	1.5
m_T	Total mass (kg)	4.3723
ω_h	Decoupled plunge natural frequency (rad/s)	27.3268
ω_α	Decoupled pitch natural frequency (rad/s)	12.11
ω_β	Decoupled control surface natural frequency (rad/s)	50.2761
x_α	Nondimensional distance between elastic axis and CG of wing	0.66
x_β	Nondimensional distance between hinge line and CG of flap	0.0028
r_α	Nondimensional rotational inertia term about elastic axis	0.7303
r_β	Nondimensional rotational inertia term about hinge line	0.0742
μ	Nondimensional mass ratio	28.3467
ζ_h	Plunge modal damping ratio	0.1275
ζ_α	Pitch modal damping ratio	0.3697
ζ_β	Flap modal damping ratio	0.0106
U_f	Linear flutter velocity (Numeric) (m/s)	11.465
U_f^*	Critical flutter velocity (Experiment) (m/s)	$12.0 \leq U_f^* \leq 12.20$

Hopf bifurcation is a typical phenomenon in nonlinear aeroelastic systems, where limit cycle oscillations (LCOs) manifest at a particular airflow velocity. This bifurcation onset can be either observed experimentally or simulated numerically. Here, numerically predicted flutter velocity for linear structural behavior is taken as the reference to compare with experimental and numerical results. The linear flutter velocity, U_f, is $11.465 m/s$ and the experimental flutter velocity,

U_f^*, is observed in the interval $12.0 < U_f^* < 12.2m/s$, thereby representing an error in between 4.45 to 6.0%. The results are given in terms of normalized numerical and experimental velocities, which are obtained dividing these velocities by $U_f = 11.465m/s$ and $U_f^* \approx 12.10m/s$, respectively, but represented as a reference to critical velocity, U_c, which is useful to compare both numerical and experimental results in the same plottings.

3.1 Hardening nonlinearity investigation

Simulations and experiments were carried out for three different intensities of the hardening nonlinearity in pitching motion as illustrated in Fig. 7(a). The hardening effects vary from large, medium, and lower increasing in restoring structural loading for the same displacement represented by the rational approximation (*cf.* Eq. (15)), where the coefficients are presented in the Tab. 2 .

Table 2. Rational polynomial coefficients for three different intensities of hardening nonlinearities.

Hardening	a_3	a_2	a_1	a_0	b_2	b_1	b_0
1	6.403	-4.76×10^{-3}	1.26×10^{-1}	-3.03×10^{-4}	1.0	2.61×10^{-7}	6.37×10^{-2}
2	6.313	-4.58×10^{-2}	3.64×10^{-2}	-2.48×10^{-4}	1.0	-1.06×10^{-2}	2.54×10^{-2}
3	7.281	3.01×10^{-2}	1.33×10^{-2}	-1.44×10^{-4}	1.0	6.39×10^{-3}	1.91×10^{-2}

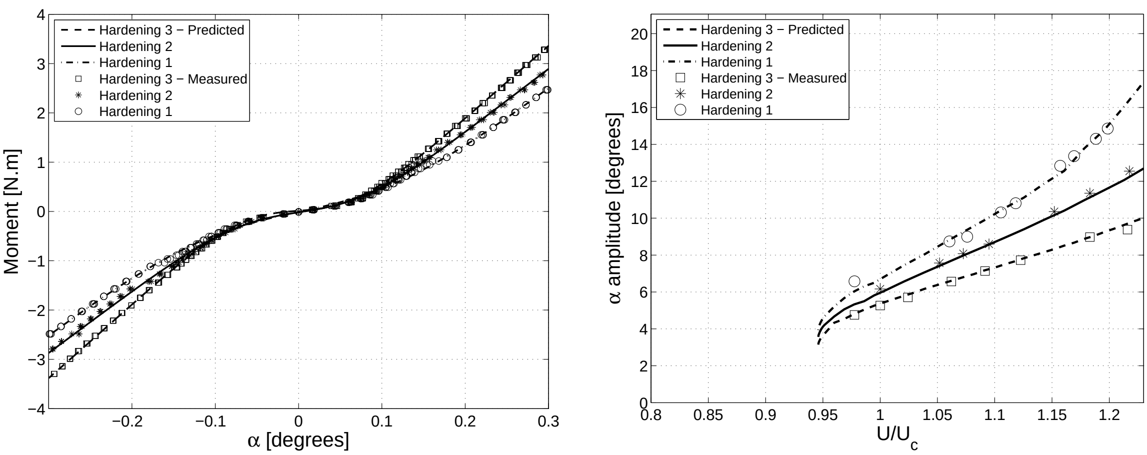

(a) Pitching moment stiffness (b) Hopf bifurcation diagram

Figure 7. Numerical and experimental results for the aeroelastic system with three different intensities of hardening nonlinearity in the pitch motion.

Figure 7(b) depict the computational and experimental results of pitching motion with no free-play in the control surface for the three different hardening effects considering increasing wind tunnel airflow velocity. The results reveal a smooth subcritical behavior, therefore, the system jumps from his fixed point stability to start LCO with high amplitude before the air velocity reaches the critical flutter speed ($U = U_c$). In the numerical results, the LCO amplitude starts with $3.2°$, $3.6°$, $3.9°$ for hardenings 3, 2, and 1, respectively, when $U = 0.945U_c$. For the experimental results, the bifurcation onset is close to $0.970U_c$, since the accuracy of the tunnel does not allow capturing the precise instability onset point.

Although the hardening nonlinearity has been responsible for the appearance of LCOs, it has not been responsible to changes in supercritical to subcritical behavior, or vice-versa. Moreover, the linear flutter velocity of the system for all LCOs starts and finishes at the same speed. The numerical results have shown good agreement with the experimental counterparts in which is possible to observe the stronger nonlinearity giving smaller LCO amplitude when the airflow velocity is increased and decreased.

3.2 Free-play nonlinearity investigation

Admitting hardening 3 nonlinearity in pitching, free-play is included to the control surface hinge. For the analysis different free-play sizes (2δ) were considered, that is, $2°$ and $4°$ (*cf.* Fig. 3(b)). The Figure 8 shows the computational and experimental results of the surface control LCO amplitudes to increasing of the airspeed. Subcritical bifurcations can be observed in all cases, but different levels of LCO amplitudes are revealed as the free-play gaps changes.

Here, it is observed that the LCOs for the computational analysis starts in the $U = 0.945U_c$, $U = 0.927U_c$, and $U = 0.917U_c$, respectively, which demonstrates that the subcritical bifurcation also increase as free-play gap size increases. The numerical results are in close agreement with the experimental data, whose results are $U = 0.977U_c$, $U = 0.958U_c$,

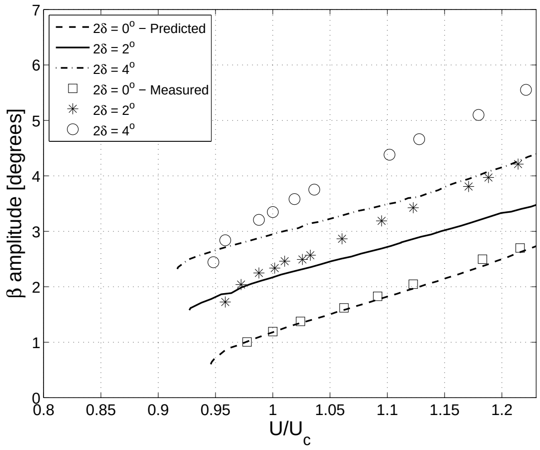

Figure 8. Hopf bifurcation diagram for the surface control displacement with hardening and free-play nonlinearity.

and $U = 0.948U_c$, respectively. Major discrepancies are observed from control surface deflections amplitudes in LCOs, with larger differences in bifurcation progress after the jump effect. Although numerical simulations indicate the need for adjustments on, perhaps, adding extra effects on free-play modeling, the results are considered satisfactory under those conditions.

3.3 Supercritical and Subcritical bifurcations analysis

Although the changes in the aeroelastic system dynamics due to structural nonlinearities, it has been observed that the linear behavior are responsible for determining whether subcritical or supercritical bifurcation occurs. To demonstrate that phenomena, the pitch moment spring stiffness has its value altered arbitrarily by increasing leading to a new $\omega_\alpha = 17.1261 rad/s$ (this corresponds to an increase of 100% in pitch stiffness). All other parameters have been left the same as in Tab. 1. The Figure 9(a) presents the bifurcation diagram for the new aeroelastic system (solid line), which results in a new critical flutter velocity of $U_f = 10.3 m/s$. One can also observe a supercritical behavior, compared with the old one (dashed line), where $\omega_\alpha = 12.11 rad/s$, for the hardening 3 and 1 present a subcritical behavior. The Figure 9(b) shows the aeroelastic system ($\omega_\alpha = 17.1261 rad/s$) when the subcritical behavior is induced by the free-play nonlinearity ($2\delta = 2°$), one can recognize that the free-play here induces a supercritical system to be a subcritical behavior as expected.

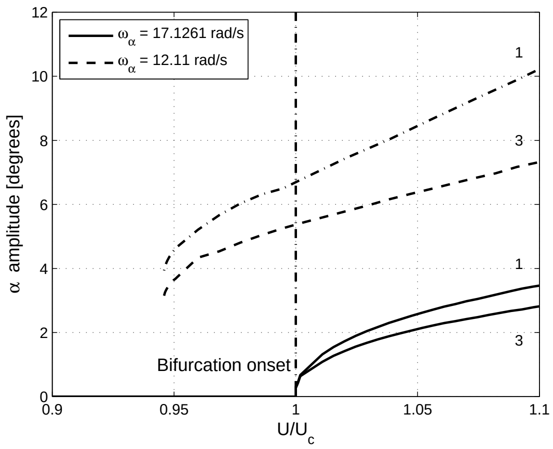

(a) Subcritical to supercritical bifurcation

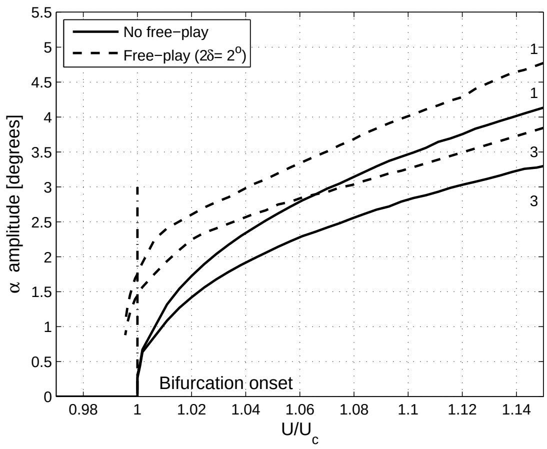

(b) Supercritical to subcritical bifurcation

Figure 9. Computational results for the aeroelastic system when the new pitch stiffness is responsible to change the Hopf bifurcation behavior.

4. CONCLUDING REMARKS

This paper has presented a study on the influence of structural nonlinearities in a three-degrees-of-freedom typical aeroelastic section using the bifurcation analysis. The computational and experimental results have focused on examining the effect of hardening in pitching motion and free-play in the control surface hinge. As observed, the hardening nonlinearity does not change the subcritical or supercritical behavior of the system, but it handles the appearance and amplitude control of LCOs. Otherwise, the free-play leads to the appearance of subcritical behavior and increase the region of dangerous LCO. In addition to that, it has also been observed the influence of the linear parameters on airfoil dynamics that determine the supercritical/subcritical behavior when the system presents only hardening nonlinearity in pitching.

Further analysis are planned to study the influence of the parameters of the system in its behavior, for instance, by changing the position of the elastic axis, CG, the moment of inertia, etc. The idea is to try to understand how they are related and how it is possible to avoid the subcritical behavior.

5. ACKNOWLEDGMENTS

The authors acknowledge the financial support of the CNPq (grant 305700/2013-8) and the Coordination for the Improvement of Higher Education Personnel (CAPES, grant 0011/07-0). The authors are also thankful to the Brazilian Research Agencies, CNPq and FAPEMIG, for funding this present research work through the INCT-EIE (National Institute of Science and Technology in Smart Structures in Engineering).

6. REFERENCES

Abdelkefi, A., Vasconcellos, R., Marques, F.D. and Hajj, M.R., 2012. “Bifurcation analysis of an aeroelastic system with concentrated nonlinearities”. *Nonlinear Dynamics*, Vol. 69, No. 1-2, pp. 57–70.

Bisphinghoff, R.L., Ashley, H. and Halfman, R.L., 1996. *Aeroelasticity*. Dover Publications.

Chen, P., Sarhaddi, D. and Liu, D., 1998. “Limit-cycle-oscillation studies of a fighter with external stores.” In *Proceedings of the 39th AIAA Structures, Structural Dynamics and Materials Conference*. Long Beach, CA, AIAA Paper 98-1727, pp. 258–266.

Denegri, C.M. and Cutchins, M.A., 1997. “Evaluation of classical flutter analyses for the prediction of limit cycle oscillations”. In *Proceedings of the 38th AIAA Structures, Structural Dynamics and Materials Conference*. Orlando, Florida, AIAA Paper 97-1021.

Dowell, E.H. and Tang, D., 2002. “Nonlinear aeroelasticity and unsteady aerodynamics”. *AIAA Journal*, pp. 40, v. 9, pp:1187–1196.

Dowell, E., Edwards, J. and Strganac, T., 2003. “Nonlinear aeroelasticity”. *Journal of aircraft*, Vol. 40, No. 5, pp. 857–874.

Ghommem, M., Hajj, M. and Nayfeh, A., 2010. “Uncertainty analysis near bifurcation of an aeroelastic system”. *Journal of Sound and Vibration*, Vol. 329, No. 16, pp. 3335–3347.

Lee, B., Gong, L. and Wong, Y., 1997. “Analysis and computation of nonlinear dynamic response of a two-degree-of-freedom system and its application in aeroelasticity”. *Journal of Fluids and Structures*, Vol. 11, No. 3, pp. 225–246.

Lee, B., Liu, L. and Chung, K., 2005. “Airfoil motion in subsonic flow with strong cubic nonlinear restoring forces”. *Journal of Sound and Vibration*, Vol. 281, No. 3, pp. 699–717.

Li, D., Guo, S. and Xiang, J., 2012. “Study of the conditions that cause chaotic motion in a two-dimensional airfoil with structural nonlinearities in subsonic flow”. *Journal of Fluids and Structures*, Vol. 33, pp. 109–126.

Li, D., Guo, S. and Xiang, J., 2010. “Aeroelastic dynamic response and control of an airfoil section with control surface nonlinearities”. *Journal of Sound and Vibration*, Vol. 329, No. 22, pp. 4756 – 4771.

Nayfeh, A.H. and Balachandran, B., 1995. *Applied Nonlinear Dynamics: Analytical Computacional, and Experimental Methods*. Wiley Series in Nonlinear Sciences. John Wiley & Sons, Inc, New York.

O’Neil, T. and Strganac, T.W., 1998. “Aeroelastic response of a rigid wing supported by nonlinear springs”. *Journal of Aircraft*, Vol. 35, No. 4, pp. 616–622.

Sears, W.R., 1940. “Operational methods in the theory of airfoils in non-uniform motion.” *Journal of the Franklin Institute*, Vol. 230, pp. 95–111.

Sheta, F., Harrand, V.J., Thompson, D.E. and Strganac, T.W., 2002. “Computation and experimental investigation of limit cicle oscillations of nonlinear aeroelastic systems”. *Journal of Aircraft*, Vol. 39, No. 1, pp. 133–141.

Theodorsen, T., 1935. “General theory of aerodynamic instability and the mechanism of flutter”. Technical Report 496, NACA Report 496.

Vasconcellos, R.M.G., Abdelkefi, A., Hajj, M.R., Almeida, D. and Marques, F.D., 2014. “Airfoil control surface discontinuous nonlinearity experimental assessment and numerical model validation”. *Journal of Vibration and Control*. Published online.

Vasconcellos, R.M.G., Abdelkefi, A., Marques, F.D. and Hajj, M.R., 2012. “Representation and analysis of control surface freeplay nonlinearity”. *Journal of Fluids and Structures*, Vol. 31, No. 6, pp. 79 – 91.

7. RESPONSIBILITY NOTICE